Type II superconducting disk in a spatially inhomogeneous applied magnetic field

M. Masale *

Department of Physics, University of Botswana, Private Bag 0022, Gaborone, Botswana

Received 27 November 2002; received in revised form 8 April 2003; accepted 15 April 2003

Abstract

The problem of a type II superconducting disk in a spatially inhomogeneous magnetic field is considered. The aim of the investigations undertaken here is to evaluate the effects of the spatial inhomogeneity of the parallel component of the applied magnetic field on the nature of the superconducting nucleation of a short cylinder. Full numerical solutions of the linearized Ginzburg–Landau equation for the order parameter, taking into account only the parallel component of the field, are presented in the case of a solid disk; free-standing and in a metallic matrix. In the case of a mesoscopic system, only the limiting form of the critical temperature is obtained. The temperature–field (ε–f) curves are characterized by flux-entry points at each of which the azimuthal quantum number decreases by unity. The quasi-period of the flux-entry points increases in f with the increasing strength of the spatial inhomogeneity of the applied field. The increased effect of coating the superconductor with a suitable normal metal leads to the well known suppression of the critical temperature as well as smoothing out of flux entries. It is predicted that the wiping out of surface nucleation is effected with relative ease when the applied magnetic field is uniform than when it posseses a degree of spatial inhomogeneity.

PACS: 74.60.Ec
Keywords: Type II superconductor; Inhomogeneous magnetic field

1. Introduction

The surface nucleation field, $H_{c3} = 1.69H_{c2}$, where H_{c2} is the bulk critical field, appears at a planar surface of a semi-infinite type II superconductor in a uniform parallel applied magnetic field [1,2]. This has also been found to be true in a thick type II superconducting film [3] and a solid cylinder [4,5] subjected to a uniform parallel magnetic field. The nature of the superconducting state just below H_{c3} depends on the dimensionless ratio of the specimen thickness to the Ginzburg–Landau (G–L) coherence length $\xi(T)$. At a critical value of the ratio, $d/\xi(T)$, where d is the thickness of the film, for example, it becomes possible for a vortex line to fit into the film. Distinct flux-entry points, which are quantized in integral multiples of the flux quantum, characterize the temperature–field curve of a type II superconducting solid cylinder in a uniform parallel applied magnetic field [4,5].

* Tel.: +267-3552940; fax: +267-585097.
E-mail address: masalem@mopipi.ub.bw (M. Masale).

Even more pronounced are the flux-entry points, known as Little–Parks oscillations, in the temperature–field curve of a very thin-walled superconducting hollow cylinder [6–8]. As in the numerous investigations [3–8] for the calculation of H_{c3}, it is sufficient to employ the G–L equation for the order parameter in its linearized form. This approximation is based on the key feature of the Landau theory of phase transitions; that near a phase transition the order parameter is very small [9]. Spatial inhomogeneities of superconducting phases can arise especially of thick specimen even in the case of a uniform applied magnetic field [10] and these should easily be accessible in micromagnetization techniques [11]. A magnetic field with a profile such as to counter spatial variations of the superconducting phases should be invaluable in the development of theoretical models. In particular, uniform nucleation of a thick specimen would mean that the system studied can be described in terms of a *constant* ground state wave function. This should, overall, ease complexities in calculations where otherwise it would be necessary to employ the full G–L equation for the order parameter, for example, as in the analysis of a superconducting cylinder as a giant vortex [12]. The modelling of a spatially inhomogeneous magnetic field which has the tendency of countering spatial variations of the superconducting phases is in essence the motivation for the investigations undertaken here.

This paper is a review of the calculation of the nucleation field of a type II superconducting cylinder. The main aim of this study is to take into account the spatial inhomogeneity of the parallel applied magnetic field. This review is based on the linearized G–L equation for the order parameter, which provides a refined approximate quantitative description of the nature of nucleation especially of filamentary specimen under the influence of weak fields [10].

The lay out of this paper is as follows: the formalism for the re-evaluation of the parallel nucleation field is outlined in Section 2. The discussion of a free-standing very short superconducting solid cylinder is given in Section 3, followed by a brief account of the effect of normal-metal cladding on the critical temperature in Section 4. The limiting form of the critical temperature of a thin-walled annular disk is discussed in Section 5 and finally, the conclusions are presented in Section 6.

2. Formalism

For the determination of the nucleation field of a type II superconductor, it is sufficient to employ the linearized G–L equation for the order parameter, ψ, given by [9]:

$$\frac{1}{2\mu}(-\imath\hbar\nabla - 2e\mathbf{A})^2\psi + \alpha\psi = 0, \tag{1}$$

where $\mathbf{A}$ is the vector potential of the applied magnetic field, μ is the mass of a particle of charge $2e$ and $\alpha = \alpha_\circ(T - T_{cb})$ is the G–L parameter in which T_{cb} is the bulk critical temperature. The general expression for the quantum mechanical current density is given by:

$$\mathbf{J} = -(\imath e\hbar/\mu)(\psi\nabla\psi - \psi\nabla\psi^\star) - (4e^2/\mu)|\psi|^2\mathbf{A}. \tag{2}$$

In the case of a free-standing superconductor or a superconductor–insulator interface, the geometry of the superconductor enters the eigenvalue problem via the boundary condition [13],

$$\hat{\mathbf{n}}\cdot(-\imath\hbar\nabla - 2e\mathbf{A})\psi = 0, \tag{3}$$

where $\hat{\mathbf{n}}$ is a unit vector normal to the interface.

3. Free-standing disk

Consider a type II superconducting short cylinder of length L_z and radius R in a static applied magnetic field with the radial B_ρ and the axial B_z components given by

$$B_\rho = \frac{B_\lambda}{\rho}\left(|z| - \frac{1}{2}L_z\right) \quad \text{and} \quad B_z = B_\mu + B_\lambda \ln(\rho/\rho_\circ), \tag{4}$$

where B_μ, B_λ and $\rho_\circ$ are constants measured in the obvious appropriate units. Although the above form of the field satisfies all the magnetostatic

equations, it is nevertheless unrealistic owing to its divergent nature at the origin. From a theoretical point of view, this singularity can be smoothed out by introducing a tiny core at the origin, or better, consider instead an annular disk. With the singularity removed, the profile of the applied magnetic field somewhat mimics that just near the ends of a magnetic dipole. Perhaps an even closer fit to the profile of the applied magnetic field can be obtained with the core of the electromagnet fashioned to have a conical end face. Note that for a concave-like core, the magnetic field lines will be concentrated near the curvature of the disk. Conversely, the concentration of the field lines will be in the inner regions of the disk if the core is convex-like. It is anticipated, however, that for a very short cylinder surface nucleation effects due B_ρ will be negligibly small, more so that $B_\rho = 0$ at the end surfaces of the disk anyway. Now, nucleation of superconductivity due to B_z is in two parts: at $B_{c\perp}$, the nucleation field perpendicular to the end faces of the disk and at B_{c3}, the critical field parallel to the curvature of the disk. Despite its variation with the radial distance, $B_{c\perp}$ is the trivial result of a type II superconducting thin film subjected to a perpendicular magnetic field. It is well known that nucleation of superconductivity occurs at a much lower temperature for the perpendicular than for the same value of the parallel applied magnetic field. Further, an increase of B_λ should give rise to an expanding normal phase of the inner region of the end faces; the expansion centered at $\rho = 0$. Arguably, nucleation of superconductivity should be increasingly localized near the edges of the end faces as the applied magnetic field is increased. In view of these considerations, the problem of the disk subjected to a magnetic field of the form given by Eq. (4) essentially reduces to that of a cylinder in a parallel magnetic field B_z, that is, the z-component of the actual applied magnetic field. Now, the logarithmic term in Eq. (4) may be represented by an approximate fitting function of the form: $\ln x \approx c_1 + c_2 x$, where c_1 and c_2 are constants which nonetheless depend on the range of the values of ρ used. These coefficients may simply be read off the computer using software packages, for example, such as grapher. Upon a renormalization of the constants B_μ, B_λ, c_1 and c_2, the actual parallel component of the magnetic field may further be approximated by the following form:

$$B(\rho) = B_o(v + \sigma\rho^2/R^2), \tag{5}$$

where B_o is the background value upon which the spatially varying part of the applied magnetic field is superimposed. The specific profile of the applied magnetic field across the cylinder radius is determined by a particular choice of the constant variables; v and σ. Although the magnetic field immediately above does not satisfy all the magnetostatic equations, it is nevertheless a very good approximation of the form that does; the field given by Eq. (4). For reasons stated earlier, it suffices to consider only the axial component of the field for the determination of the required critical field. Taken only with one component in the azimuthal direction, the vector potential associated with the approximate form of the magnetic field above may be written as

$$A_\varphi = \frac{1}{2}B_o\left(v\rho + \frac{1}{2}\sigma\rho^3/R^2\right). \tag{6}$$

In view of the symmetry of the problem posed here, the solution of Eq. (1) is sought in the form:

$$\psi = C_{m\ell}\exp(im\phi)\chi, \quad m = 0, \pm1, \pm2\ldots, \tag{7}$$

where $C_{m\ell}$ is a constant, m the azimuthal quantum number and χ is the radial part of the total wave function, taken in the transformation:

$$\chi = \zeta^{|m|/2}\exp(-\zeta/2)\mathscr{F}. \tag{8}$$

The dimensionless variable ζ is defined by $\zeta = \rho^2/2a_{oc}^2$, in which $a_{oc} = (\hbar/2eB_o)^{1/2}$ is the cyclotron radius corresponding to the background magnetic field B_o. The function $\mathscr{F}$ is found to satisfy the following linear second-order differential equation:

$$\zeta\mathscr{F}'' + [b - \zeta]\mathscr{F}' - [a + h(\zeta)]\mathscr{F} = 0, \tag{9}$$

where the primes on $\mathscr{F}$ denote differentiation of the function with respect to the argument ζ. The parameters a and b are:

$$a = \frac{1}{2} + \frac{1}{2}|m| + \frac{1}{2}mv - \frac{1}{2}\frac{\varepsilon}{f_o}, \quad b = |m| + 1 \tag{10}$$

and the function $h(\zeta)$ is given by

$$h(\zeta) = \frac{1}{4}\left[v^2 - 1 + \frac{1}{2}\frac{m\sigma}{f_o}\right]\zeta + \frac{1}{8}\frac{v\sigma}{f_o}\zeta^2 + \frac{1}{64}\frac{\sigma^2}{f_o^2}\zeta^3. \tag{11}$$

The dimensionless variables ε and f_o are defined by the following relationships:

$$\varepsilon = \mu|\alpha|R^2/2\hbar^2 \quad \text{and} \quad f_o = \pi B_o R^2/2\phi_o = R^2/4a_{oc}^2. \tag{12}$$

Note that for $v = 1$ and $\sigma = 0$, Eq. (9) reduces to Kummer's equation for the confluent hypergeometric function, that is, $\mathscr{F} = M(a, b, \zeta)$. This is in fact the special case of a cylinder in a uniform applied magnetic field, say B_o. Eq. (9) was solved by the series method, obtaining the function $\mathscr{F}$ as well as its first derivative $\mathscr{F}'$ each in terms of a four-term recursion relationship for the coefficients of ζ. Algorithms were developed for the evaluations of the functions $\mathscr{F}$ and M based on their series representations. The confidence level regarding the trustworthy of the numerical evaluations of $\mathscr{F}$ was pivoted on the two limiting forms that: $\mathscr{F} \sim M$ as $\zeta \to 0$ and $\mathscr{F} \to M$ as $\sigma \to 0$, for all ζ. Conversion of the series is fast and almost guaranteed for $a < 0$ particularly for small ζ although it has to be said that a higher number of terms are required to achieve in the case of $\mathscr{F}$. Equipped with subroutines for the evaluations of $\mathscr{F}$ and $\mathscr{F}'$, generating the field–temperature curves is then a matter of standard routine: first fix f_o, then search for the negative fluxoid number m which gives the lowest value of ε. Only the minimum value of ε has physical significance since it is the one that corresponds to the required critical field.

The application of the boundary condition at the surface of a free-standing disk, which in this case simplifies to $\frac{d\psi}{d\rho} = 0$ for $\rho = R$, leads to the following eigenvalue equation:

$$(|m| - 2f_o)\mathscr{F}(v, \sigma, a, b, 2f_o) + 4f_o\mathscr{F}'(v, \sigma, a, b, 2f_o) = 0. \tag{13}$$

For a disk of thickness such that $R < \xi(T)$, there can hardly be any phase changes of ψ, even in the case when the applied magnetic field varies spatially. The derivatives of ψ vanish and the small f_o limiting form of ε obtained from integrating Eq. (1) across the radius of the disk is found as:

$$\varepsilon_o = \frac{1}{2}m^2 + \left[v + \frac{1}{3}\sigma\right]mf_o + \left[\frac{2}{3}v^2 + \frac{1}{2}v\sigma + \frac{1}{10}\sigma^2\right]f_o^2. \tag{14}$$

The simple result above is helpful mainly as a guide to the full numerical solutions of Eq. (9). Now, the definition of f_o given by Eq. (12) is essentially the magnetic flux of a uniform magnetic field B_o penetrating the cross-sectional area of the cylinder per twice the flux quantum. Indeed f_o is a convenient parameter with which to represent a uniform magnetic field. However, a complication arises in the case of a spatially inhomogeneous applied magnetic field. While the short cylinder as a whole responds to the flux through it, the value of the field at the curved surface may not necessarily correspond to H_{c3}, for example, when $v + \sigma = 0$. Two useful representations of the inhomogeneous field are as follows:

$$f_s = f_o(v + \sigma), \tag{15}$$

which is defined in terms of the value of the magnetic field at the surface of the cylinder, namely $B_s = B_o(v + \sigma)$. This representation is more appropriate for the calculation of H_{c3} but has no bearing on the nature of the superconducting phases of the interior regions of the cylinder. The second representation, analogous to the definition of f_o given by Eq. (12) is defined by

$$f = \frac{1}{2\phi_o}\int \mathbf{B}\cdot d\mathbf{S} = \left(v + \frac{1}{2}\sigma\right)f_o, \tag{16}$$

that is, is in terms of the actual flux through the axial area $\mathbf{S}$ of the cylinder. This representation prescribes nucleation of a cylinder as a whole and is arguably more suitable for very fine superconducting filaments. As noted earlier, spatial variations of the magnetic field in a cylinder of very small radius are hardly significant. It is convenient, especially in connection with the first of these representations of the field given by Eq. (15), to impose the constraint that $v + \sigma = 1.0$ and such that $v > 0$. First, this restriction on the values of v and σ avoids complicated profiles of the applied field across the cylinder thickness, for example, a

change of sign of the applied field within the cylinder radius. Second, the results obtained here then directly relate to the special case of a cylinder in a uniform magnetic field.

Fig. 1 shows the temperature–field curves in the two representations mentioned above for some few values of v or $\sigma = 1 - v$. To be more specific, Fig. 1a is a plot of ε versus $f_s(= f_o)$ and Fig. 1b that of ε versus f. Each curve in either of the two plots corresponds to a different value of v, at say $f = f_s = 5.0$, as follows: Fig. 1a; $v = 1.0$ for the lowest (thick) curve, increasing in steps of $\Delta v = 0.2$ up to $v = 2.0$, for the highest curve. The stacking up of the curves at $f = 5.0$ in Fig. 1b is in the reverse order of the increasing values of v given above. The thick curve in each plot is the result for the special case of a uniform applied magnetic field. Just like in the case of a superconducting solid cylinder in a uniform magnetic field [4,5], each curve consists of joint segments each corresponding to unit stepwise decrease of m as the field increases. The striking feature of Fig. 1a is the fanning-out of the ε–f_s curves for the different values of v, giving the false impression of the suppression of the critical temperature as v increases. As such, the fanning-out of the curves for the different values of v is a consequence of underestimating the flux penetrating the axial area of the cylinder, in fact by a factor $\gamma = \frac{1}{2}[v + 1]$. It is interesting to note that the $\sigma \neq 0$ curves in the representation of Fig. 1b are merely displaced relative to the universal temperature–field curve for the special case of a uniform applied magnetic field. In Fig. 1b, as v is increased, the cusps of the non-zero σ curves shift slightly towards the origin, essentially along the universal temperature–field curve for uniform applied magnetic field. A case can therefore be made for the representation of Fig. 1b as the one that depicts the true universal temperature–field curve of a superconductor in a non-uniform applied magnetic field.

The nature of the superconducting phase across the cylinder thickness may be inferred from the spatial variations of the radial wave functions or

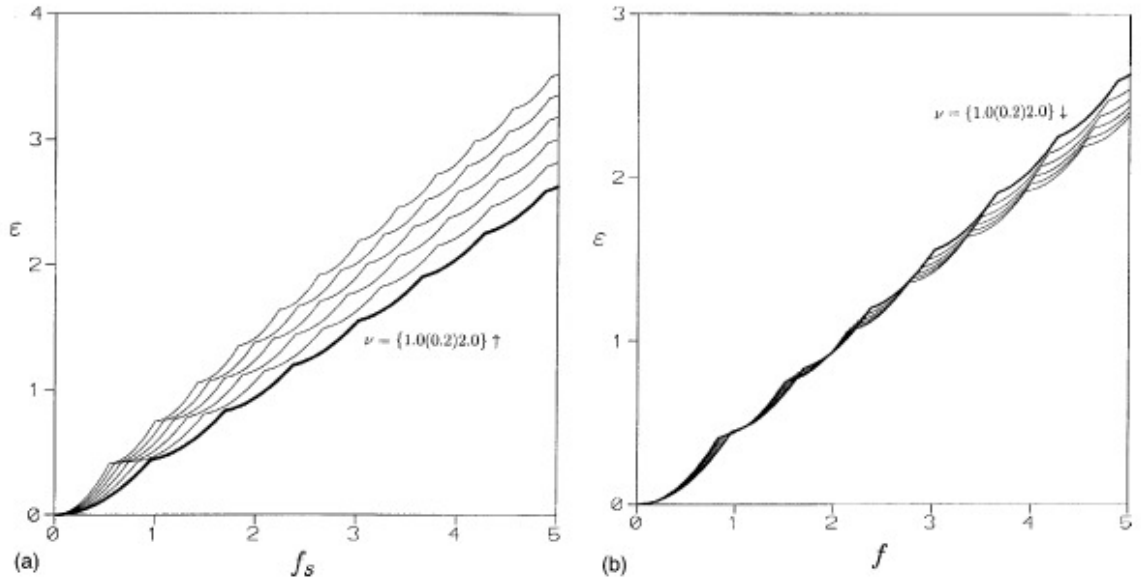

Fig. 1. (a) The ε versus f_s curves of a type II superconducting disk in a spatially inhomogeneous axial magnetic field. Each curve corresponds to a different value of v, ranging from 1.0 and increasing in steps of $\Delta v = 0.2$, in the direction of the arrow, up to 2.0. The thick lowest curve is the result for the special case of a uniform applied magnetic field corresponding to $v = 1.0$. (b) The universal critical field–temperature (ε–f) curves of type II superconducting disk for exactly the same values of v as for Fig. 1a. Here the field is represented in terms of the actual flux through the disk. Note also that here these curves stack-up, at say $f = 5.0$, according to the decreasing values of v used.

the current density across the thickness of the cylinder. The explicit form of the current density is found to be

$$\frac{J_\phi}{J_{o\phi}} = -(|m| + [2v + \sigma x^2]fx^2)\chi(\rho)^2/x, \tag{17}$$

where $x = \rho/R$ and $J_{o\phi} = 2e\hbar/(\mu R)$.

The variations of the $v \neq 0$ radial wave functions are very similar to those in the investigations by Constantinou et al. [5] and are only shown here for the sake of completeness. Fig. 2 compares the radial wave functions corresponding to $v = 2.0$, the solid curves, with those obtained in the case of a uniform magnetic field, $v = 1.0$, shown as the broken lines. The corresponding (f, m) values, at say, $\rho/R = 0.5$ are: (0.5,0) for the topmost pair of curves, (1.5,−1) for the middle pair and (2.5,−3) for the lowest pair of curves. For convenience, the wave functions have been normalized by their respective values for $\rho = R$. For small f, as confirmed by the curves corresponding to $f = 0.5$, there can hardly be any spatial variations of the wave function. This implies that nucleation of superconductivity is uniform in filamentary wires despite the spatial variations of the applied magnetic field. As f increases, however, phase changes of the wave function become significant. For example, the wave function corresponding to $f = 2.5$ is very small for regions in the interior of the cylinder, assuming a maximum value at the surface. This implies the presence of a superconducting sheath at the surface while the bulk of a thick cylinder is in the normal phase.

Fig. 3 compares the current densities across the cylinder radius corresponding exactly to the wave functions depicted in Fig. 2. The corresponding (f, m) values are: (0.5,0) for the lowest pair of curves, (1.5,−1) for the middle pair and (2.5,−3) for the highest pair of curves. The build-up of the current densities near the cylinder-surface for the two types of the magnetic field profiles considered confirms the presence of surface nucleation. However, note the dipping at the surface of the curves for the case of an inhomogeneous magnetic field, which is more pronounced for large values of f. It should be mentioned that in contrast to the spatial variations of the wave functions, a decrease

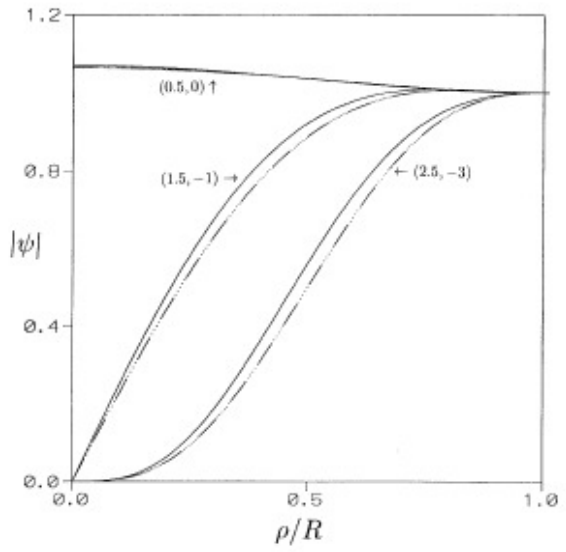

Fig. 2. The variations of some few radial wave functions across the radius of the disk. The dashed curves with dots are for the special case of a uniform magnetic field such that $v = 1.0$. The corresponding results for a spatially inhomogeneous applied magnetic field corresponding to $v = 2.0$ are depicted as the solid lines. The (f, m) values for each corresponding pair of curves, indicated there are: (0.5,0) for the topmost pair, (1.5,−1) for the middle pair and (2.5,−3) for the lowest pair.

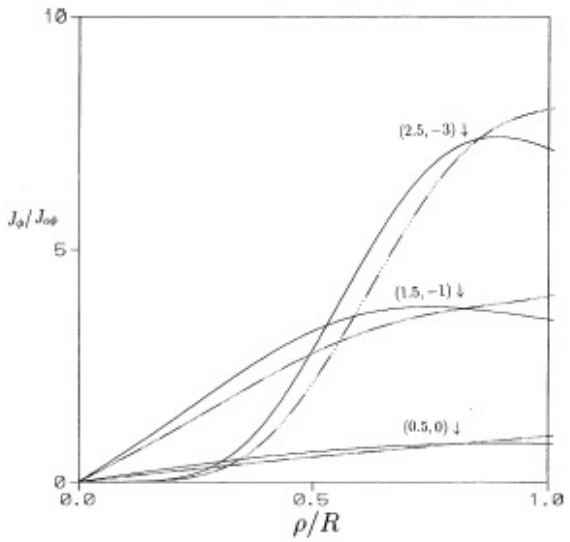

Fig. 3. The distribution of the quantum mechanical current density across the radius of the disk corresponding exactly to the wave functions shown in Fig. 2.

of the current density is indicative of the onset of superconductivity. The dipping of J at $\rho = R$ therefore implies a pseudo return to the superconducting phase there. This is consistent with the decrease of the applied magnetic field as ρ ($\leqslant R$) increases.

4. Disk in a metallic matrix

Surface nucleation is suppressed if a superconductor is coated with a suitable normal conductor. This is accompanied by the systematic depression of the order parameter at the surface of a superconductor. The extent of the depression is such that the slope of the wave function at the surface can be extrapolated to the value, ψ/δ, where the doping-controlled parameter δ is the extrapolation length. In the case of a superconducting solid cylinder in a metallic matrix, the condition of a zero-gradient at the boundary is replaced by [13]:

$$\frac{\mathrm{d}\psi}{\mathrm{d}\rho} + \frac{\psi}{\delta} = 0. \tag{18}$$

The application of the boundary condition above leads to the following eigenvalue equation:

$$[|m| - 2f_\circ + R/\delta]\mathscr{F}(v,\sigma,a,b,2f_\circ) + 4f_\circ\mathscr{F}'(v,\sigma,a,b,2f_\circ) = 0. \tag{19}$$

The effects of normal-metal cladding on the critical temperature of superconductors with cylindrical symmetry has been discussed extensively in a number of publications [4,5,8,10]. A brief discussion of normal-metal cladding is given, highlighting only the features brought about by the inhomogeneity of the applied magnetic field.

Fig. 4 shows the effect of metallic cladding on the variation of the critical temperature (ε) with the field (f) corresponding to $v = 2.0$. The increasing suppression of the critical temperature T_c for zero magnetic field corresponds to the increasing values of the ratio R/δ as follows: 0.0 for the lowest curve, increasing steps of 2.0 up to 10.0 for the highest curve. Of course, the zero-field variation of ε with R/δ is in exact agreement with the results reported previously [8]. For large values of f, the degree of the suppression of T_c is significantly higher here than in the case of a uniform applied magnetic field. As in the case of a cylinder in a uniform magnetic field, the number of flux-entry points of the ε–f curve decreases with the increase of R/δ which signifies the wiping out of surface nucleation. In this case, complete suppression of surface nucleation, when $\varepsilon \sim f$ and corresponding to $m = 0$, occurs at higher values of R/δ than in the case of the cylinder in a uniform applied magnetic field. This is what might be anticipated should the superconducting sheath in this case be thicker than one for a cylinder in a uniform magnetic field.

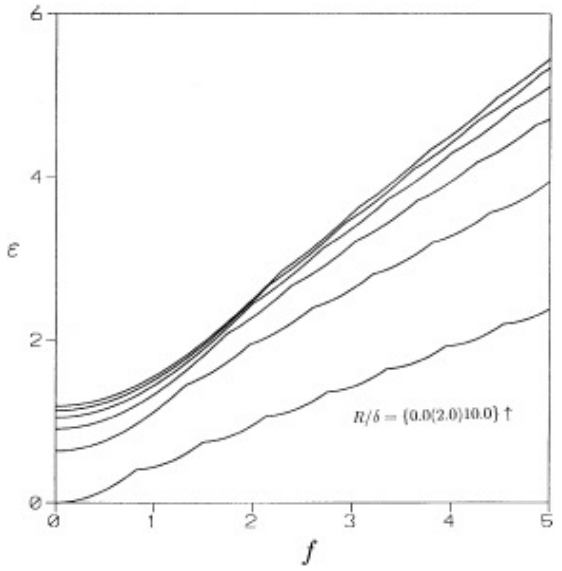

Fig. 4. The universal critical field–temperature curves of disk in a non-superconducting metallic matrix. The intercepts increase according to the values of the extrapolation length such $R/\delta = 0.0$ for the lowest curve, increasing in steps of $\Delta(R/\delta) = 2.0$ up to $R/\delta = 10.0$ for the highest curve.

5. Free-standing mesoscope

The system considered here is a free-standing very short and thin-walled hollow cylinder of inner and outer radii R_1 and R_2, respectively. The applied inhomogeneous magnetic field is again assumed to have the form given by Eq. (5). As stated earlier, there can hardly be spatial variations of the

order parameter across a superconductor of thickness much smaller than the G–L coherence length. Further, for such small thicknesses, monotonic spatial variations of the applied inhomogeneous magnetic field are too weak to induce phase changes of the order parameter. Following Masale et al. [8], the limiting form of the critical temperature, obtained on integrating the G–L in χ across the shell thickness is given by:

$$\varepsilon_2 = \frac{1}{2}m^2\frac{1}{1+\eta} + pmf_{o2} + qf_{o2}^2, \tag{20a}$$

where

$$p = v + \tfrac{1}{3}[1-\eta^3][1-\eta^2]^{-1}\sigma \tag{20b}$$

and

$$q = \frac{2}{3}\left([1-\eta^3][1-\eta^2]^{-1}\right)v^2 + \frac{1}{2}[1+\eta^2]v\sigma + \frac{1}{10}\left([1-\eta^5][1-\eta^2]^{-1}\right)\sigma^2, \tag{20c}$$

in which $\eta = R_1^2/R_2^2$. The numeral subscript on ε and f_o indicates that the definitions of the respective variables are in terms of R_2. The inhomogeneous field is represented in terms of the actual flux penetrating the thickness of the shell according to:

$$f_2 = f_{o2}[1-\eta]\left(v + \tfrac{1}{2}[1+\eta]\sigma\right). \tag{21}$$

Note that unlike in the investigations very closely related to one undertaken here, the representation of the field given by Eq. (21) excludes the so-called missing flux;

$$\Phi_1 = \pi B_o R_1^2\left(v + \tfrac{1}{2}\sigma\right), \tag{22}$$

this being the flux through the hole.

Fig. 5 compares the ε_2–f_2 curves of a thin-walled short hollow cylinder of thickness such that $\eta = 0.5$ for two specific profiles of the magnetic field. The dashed curve is for the case of a shell in a uniform magnetic field, that is, for $v = 1.0$. The smooth solid curve is the result for the shell in an inhomogeneous such that $v = 2.0$. Each of the two curves is characterized by strong oscillations of the critical temperature in its variation with the field. This quasi-periodic variation, known as Little–Parks oscillation, is superimposed on a slow overall decrease of T_c. Each period corresponds to an increase by unity in the fluxoid number

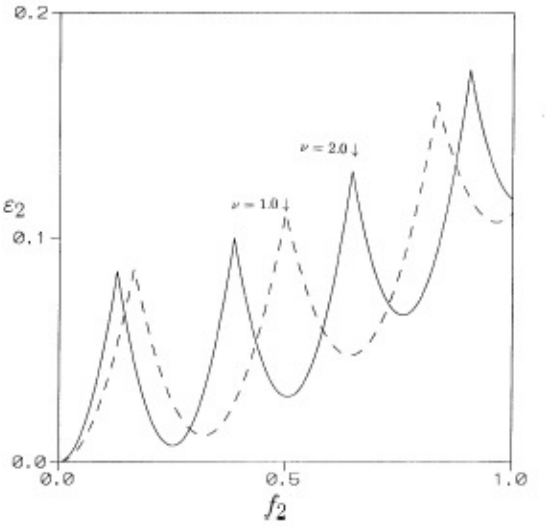

Fig. 5. The ε_2 versus f_2 curves of a short and thin-walled type II superconducting hollow cylinder of thickness such that $\eta = 0.5$. The dashed curve is for the case of a shell in a uniform magnetic field. The smooth solid curve is the result for the shell in an inhomogeneous magnetic field such that $v = 2.0$.

enclosed within the shell-thickness. Just like in the earlier discussion of a short solid cylinder, the inhomogeneity of the applied magnetic field manifests itself in the relative shifting of flux entries to smaller values of ε_2 and f_2. Again, the displacement of the uniform-field universal curve towards smaller values of ε_2 and f_2 is a consequence of underestimating the flux penetrating the shell-thickness. It is worth mentioning that overestimating the flux through the shell, as in the representation of the field as f_{o2}, leads to a dramatic "upward" shift of the flux-entry points as the field is increased. This is marked by a drastic reduction in the number of flux-entry points on the universal temperature–field curve, consistent with the suppression of spatial variations of the superconducting phases across the specimen.

6. Conclusions

The linearized G–L equation for the order parameter was employed in the description of the Meissner effect of a type II superconducting short cylinder in a spatially inhomogeneous applied

magnetic field. Overall, the applied magnetic field consisted of a part with a parabolic variation in the radial distance, this being superimposed on a constant background value. Two sets of plots of the critical temperature–field curves of a disk were generated in which the field was represented either in terms of the flux corresponding to the background value of the magnetic field; Fig. 1a; or in terms of the actual flux penetrating the axial area of the disk; Fig. 1b. Just like in the case of a cylinder in a uniform parallel applied magnetic field, the temperature–field curves are characterized by a succession of distinct flux-entry points at each of which m decreases by unity. Cusps, each corresponding to a particular m are much more pronounced in the case of a very thin-walled annular disk. These appear as a series of quasi-periodic segments joined end to end and are referred to as Little–Parks oscillations. In the first of these representations, the ε–f_s curves for the different "strengths" ($|\sigma|$) of the parabolic part of the field fan-out as the background value of the applied magnetic field is increased. Increasing $|\sigma|$ essentially resulted in an anticlockwise rotation of the uniform-field universal temperature–field curve about the origin. This false impression of the depression of the critical temperature is a consequence of underestimating the flux through the cylinder. In the second of these representations, as in Fig. 1b, increasing $|\sigma|$ leads merely to a displacement of the uniform-field universal ε–f curve towards the origin. This displacement, accompanied by a slight apparent clockwise rotation, of the ε–f curve is seen in the decrease of the flux-entry points within the given range of the values of f used. It was noted that even in the case of the spatially inhomogeneous applied magnetic field, the superconducting phase nucleates uniformly across a disk of small radius. A superconducting sheath persists at the surface while the inner region of wide pill-box is in the normal state. The current densities corresponding to $\sigma \neq 0$, particularly for large f, posses maxima near the surface of the cylinder in their variations with the radial distance. The dipping of the current densities, which arises as a consequence of the inhomogeneity of the applied magnetic field, is believed to indicate an increased stability of the superconducting phase there, at least in comparison with the case of a cylinder in a uniform magnetic field. Finally, metallic cladding was found to show the well known effects of the suppression of the critical temperature as well as surface nucleation. The suppression of surface nucleation is seen in the wiping out of flux-entry points, which are seen to progress to higher values of ε and f as R/δ is increased. Complete suppression of surface nucleation is achieved at much lower values of R/δ in the case of the cylinder in a uniform magnetic field than in the corresponding case of the spatially inhomogeneous magnetic field.

References

[1] D. Saint-James, P.G. de Gennes, Phys. Lett. 7 (1963) 306.
[2] S. Gygax, R.H. Kropschot, Phys. Lett. 9 (1964) 91.
[3] E. Guyon, F. Meunier, R.S. Thompson, Phys. Rev. 156 (1967) 452.
[4] S. Takács, Czech J. Phys. 19 (1969) 1366.
[5] N.C. Constantinou, M. Masale, D.R. Tilley, J. Phys C.: Condens. Matter 4 (1992) L293.
[6] W.A. Little, R.D. Parks, Phys. Rev. Lett. 9 (1962) 9.
[7] H.J. Fink, V. Grünfeld, Phys. Rev. B 22 (1980) 2289.
[8] M. Masale, N.C. Constantinou, D.R. Tilley, Supercond. Sci. Technol. 6 (1993) 287.
[9] D.R. Tilley, J. Tilley, Superfluidity and Superconductivity, Bristol, Hilger, 1990.
[10] M. Masale, Physica C 377 (2002) 75.
[11] A.K. Geim, I.V. Grigorieva, J.G.S. Lok, J.C. Maan, S.V. Dubonos, X.Q. Li, F.M. Peeters, Yu.V. Nazarov, Superlatt. Microstruct 23 (1998) 151.
[12] H.J. Fink, A.G. Presson, Phys. Rev. 151 (1966) 219.
[13] P.G de Gennes, Superconductivity of Metals and Alloys, Benjamin, New York, 1966.